Novel ^{64}Cu- and ^{68}Ga-Labeled RGD Conjugates Show Improved PET Imaging of $\alpha_v\beta_3$ Integrin Expression and Facile Radiosynthesis

Rebecca A. Dumont[1], Friederike Deininger[1], Roland Haubner[2], Helmut R. Maecke[1], Wolfgang A. Weber[1], and Melpomeni Fani[1]

[1]*Department of Nuclear Medicine, University Hospital Freiburg, Freiburg, Germany; and* [2]*Department of Nuclear Medicine, Innsbruck Medical University, Innsbruck, Austria*

PET with ^{18}F-labeled arginine-glycine-aspartic acid (RGD) peptides can visualize and quantify $\alpha_v\beta_3$ integrin expression in patients, but radiolabeling is complex and image contrast is limited in some tumor types. The development of ^{68}Ga-RGD peptides would be of great utility given the convenience of ^{68}Ga production and radiolabeling, and ^{64}Cu-RGD peptides allow for delayed imaging with potentially improved tumor-to-background ratios. **Methods**: We used the chelators DOTA,1,4,7-triazacyclononane,1-glutaric acid-4,7-acetic acid (NODAGA), and 4,11-bis(carboxymethyl)-1,4,8,11-tetraazabicyclo[6.6.2] hexadecane (CB-TE2A) to radiolabel the cyclic pentapeptide c(RGDfK) with ^{68}Ga or ^{64}Cu. NODAGA-c(RGDfK) was labeled at room temperature with both radionuclides within 10 min. Incubation at 95°C for up to 30 min was used for the other conjugates. The affinity profile of the metallopeptides was evaluated by a cell-based receptor-binding assay. Small-animal PET studies and biodistribution studies were performed in nude mice bearing subcutaneous U87MG glioblastoma xenografts. **Results:** The conjugates were labeled with a radiochemical purity greater than 97% and specific activities of 15–20 GBq/μmol. The affinity profile was similar for all metallopeptides and comparable to the reference standard c(RGDfV). In the biodistribution studies, all compounds demonstrated a relatively similar tumor and normal organ uptake at 1 h after injection that was comparable to published data on ^{18}F-labeled RGD peptides. At 18 h after injection, however, ^{64}Cu-NODAGA-c(RGDfK) and ^{64}Cu-CB-TE2A-c(RGDfK) showed up to a 20-fold increase in tumor-to-organ ratios. PET studies demonstrated high-contrast images of the U87MG tumors at 18 h, confirming the biodistribution data. **Conclusion:** The ease of radiolabeling makes ^{68}Ga-NODAGA-c(RGDfK) an attractive alternative to ^{18}F-labeled RGD peptides. The high tumor-to-background ratios of ^{64}Cu-NODAGA-c(RGDfK) and ^{64}Cu-CB-TE2A-c(RGDfK) at 18 h warrant testing of ^{64}Cu-labeled RGD peptides in patients.

Key Words: ^{68}Ga PET/CT; ^{64}Cu PET/CT; RGD conjugates; angiogenesis; integrins

J Nucl Med 2011; 52:1276–1284
DOI: 10.2967/jnumed.111.087700

During the last 12 y, a variety of imaging probes have been developed that target the $\alpha_v\beta_3$ integrin (*1*). The strong interest in imaging the expression and functional activity of this molecule stems from its important role in several common diseases. The $\alpha_v\beta_3$ integrin is an adhesion molecule that mediates migration of cells on the extracellular matrix. In addition, it acts as a receptor that senses the interaction of cells with the extracellular matrix and activates intracellular signaling pathways. The $\alpha_v\beta_3$ integrin is expressed on activated endothelial cells during angiogenesis, whereas resting endothelial cells show only low expression levels of this receptor. Increased $\alpha_v\beta_3$ expression has been observed in intratumoral blood vessels, new blood vessels formed after myocardial infarction, and blood vessels in chronic inflammatory processes (*2,3*). Furthermore, the $\alpha_v\beta_3$ integrin is expressed by some cancer cells, such as glioblastoma and melanoma, and facilitates invasiveness and metastasis formation. Thus, imaging of $\alpha_v\beta_3$ expression has many applications for studies in oncology, cardiology, and inflammatory diseases (*2,3*).

Initial studies used MRI and antibody-coated paramagnetic liposomes to image $\alpha_v\beta_3$ expression in animal tumors (*4*). Subsequent work has focused on cyclic pentapeptides based on the lead structure cyclo(Arg-Gly-Asp-D-Phe-Val) (*1*). These peptides have been radiolabeled for SPECT and PET but also used for contrast-enhanced MRI and ultrasound studies. These extensive preclinical studies have demonstrated that the $\alpha_v\beta_3$ integrin is a promising target for imaging of angiogenesis and tumor cell invasiveness (*1,5*). Clinical studies are most advanced for PET with the glycosylated peptide ^{18}F-galacto-RGD (arginine-glycine-aspartic acid) (*6*). $\alpha_v\beta_3$ expression has been imaged in a variety of malignant tumors including melanomas, sarcomas,

Received Jan. 12, 2011; revision accepted Apr. 20, 2011.
For correspondence or reprints contact: Melpomeni Fani, Department of Nuclear Medicine, University Hospital Freiburg, Hugstetterstrasse 55, D-79106 Freiburg, Germany.
E-mail: melpomeni.fani@uniklinik-freiburg.de

and head and neck cancer using this peptide (*7*). Other ^{18}F-labeled RGD peptides in clinical trials include ^{18}F-AH111585 and ^{18}F-RGD-K5 (*8,9*). These clinical studies have shown that PET with radiolabeled RGD peptides can be used to detect $\alpha_v\beta_3$-expressing tumors in patients and quantitatively evaluate the expression levels of $\alpha_v\beta_3$ integrins.

The clinical studies have also revealed important limitations of PET with ^{18}F-RGD peptides. In several cases, image contrast is suboptimal, limiting the detection and characterization of small lesions or lesions with moderate $\alpha_v\beta_3$ integrin expression levels. Furthermore, radiolabeling with ^{18}F is relatively complex (especially for ^{18}F-galacto-RGD), making large-scale clinical studies challenging. Thus, the clinical use of RGD peptides would clearly be enhanced by new probes that are less complex to radiolabel and provide higher image contrast than currently available compounds.

In this study, we examined whether these 2 requirements can be fulfilled by RGD peptides labeled with radiometals. For this purpose, we coupled an RGD peptide to chelators that stably bind ^{68}Ga or ^{64}Cu in vivo. These chelators allow for efficient and straightforward labeling procedures. In addition, the 12.7-h half-life of ^{64}Cu enables delayed imaging with potentially increased image contrast.

MATERIALS AND METHODS

General

All commercially obtained chemicals were of analytic grade and were purchased from common suppliers. 2-chlorotrityl chloride resin and 9-fluorenylmethoxycarbonyl (Fmoc) amino acids were purchased from NovaBiochem AG and Bachem. $^{64}CuCl_2$ was produced at the University Hospital of Tübingen. A ^{68}Ge/^{68}Ga generator (1,110 MBq) was obtained from Eckert & Ziegler. ^{125}I-echistatin (81,400 GBq [2,200 Ci]/mmol) was purchased from PerkinElmer. c(RGDfV) was purchased from Bachem. All reagents used in cell cultures were purchased from Gibco (Invitrogen). The reversed-phase high-performance liquid chromatography (RP-HPLC) systems, γ-counter, and electrospray ionization mass spectrometer were the same as previously reported (*10*). The HPLC gradient was 0–25 min 95%–50% A (A, 0.1% trifluoroacetic acid in water; B, acetonitrile); flow rate, 1 mL/min; and column, Macherey-Nagel, Nucleosil 120-C_{18}.

Peptide–Conjugate Synthesis

The orthogonally protected linear H-Asp(OtBu)-D-Phe-Lys (ivDde)-Arg(Pbf)-Gly-OH (RGDfK), where tBu is *tert*-butyl, ivDde is 1-(4,4-dimethyl-2,6-dioxocyclohexylidene)-3-methyl-butyl, and Pbf is 2,2,4,6,7-pentamethyl-dihydrobenzofuran-5-sulfonyl, was synthesized by standard Fmoc solid-phase synthesis on 2-chlorotrityl chloride resin (1.3 mmol/g). Fmoc-Gly-OH was initially attached to the resin using 4 equivalents of ethyldiisopropylamine (DIPEA). Couplings were then performed with 3 equivalents of each of the other amino acids and mediated by 3 equivalents of 1-hydroxybenzotriazole (HOBt) and 3 equivalents of *N,N′*-diisopropylcarbodiimide (DIC), along with 6 equivalents of DIPEA for 1–2 h. Fmoc removal was achieved with 20% piperidine in *N,N*-dimethylformamide (DMF). The peptide was cleaved from the resin with a mixture of acetic acid/2,2,2-trifluoroethane/dichloromethane 1:1:3. Head-to-tail cyclization took place in solution at room temperature (RT) overnight, after the addition of 50% 1-propanephosphonic acid cyclic anhydride in ethylacetate, triethylamine, and 4-di(methylamino) pyridine, as previously described (*11*). The protected cyclic peptide was purified on a Silica gel 60 column (ethyl acetate/methanol 9:1). The ivDde group was removed from the ε-amino group of Lys with 2% hydrazine in DMF. The prochelators 2-(4,7,10-tris(2-tert-butoxy-2-oxoethyl)-1,4,7,10-tetraazacyclododecan-1-yl) acetic acid (DOTA(tBu)) (Chematech), 1-(1-carboxy-3-carbo-*tert*-butoxypropyl)-4,7-(carbo-*tert*-butoxymethyl)-1,4,7-triazacyclononane (NODAGA(tBu)$_3$) (synthesized according to the literature (*12*)), or 2-(11-(2-(tert-butoxy)-2-oxoethyl)-1,4,8,11-tetraazabicyclo[6.6.2] hexadecan-4-yl)acetic acid (CB-TE1A1A(tBu) (synthesis will be published elsewhere) were coupled in solution using 1 equivalent of each prochelator, 1 equivalent of 2-(7-aza-1H-benzotriazole-1-yl)-1,1,3,3-tetramethyluronium hexafluorophosphate, and 2 equivalents of DIPEA in DMF for 3–4 h. All side-chain–protecting groups were then removed with a cocktail of trifluoroacetic acid/thioanisol/triisopropylsilan/water 95:3:1:1. The crude product was purified by preparative HPLC and identified by electrospray mass spectrometry.

Preparation of ^{64}Cu and ^{68}Ga Radiotracers and Cold Complexes

^{64}Cu-labeled conjugates were prepared after incubation of 5–10 μg of each conjugate, with 37–74 MBq of $^{64}CuCl_2$ in ammonium acetate buffer (0.1 mol/L, pH 8.0). CB-TE2A-c(RGDfK) and DOTA-c (RGDfK) were labeled at 95°C within 30 min, and NODAGA-c (RGDfK) was labeled at RT within 10 min. ^{68}Ga-labeled conjugates were prepared using the Modular-Lab PharmaTracer module by Eckert & Ziegler. Briefly, the ^{68}Ge/^{68}Ga generator was eluted with 7 mL of HCl 0.1N, and the eluate (240–290 MBq) was loaded onto a cation exchange column (Strata-XC; Phenomenex). ^{68}Ga was eluted with 800 μL of a mixture of acetone/HCl (97.6%/0.02N) directly in a vial containing 2 mL of sodium acetate buffer (0.2 mol/L, pH 4.0) and 10 μg of the conjugate. DOTA-c(RGDfK) was labeled at 95°C within 8 min and NODAGA-c(RGDfK) at RT within 10 min. Quality control was performed by RP-HPLC. The radiotracer solutions were prepared by dilution with 0.9% NaCl.

For the preparation of the metallopeptides, a 2-fold excess of $^{nat}CuCl_2 \times 2\ H_2O$ or $^{nat}Ga(NO_3)_3 \times H_2O$ was used under the same conditions used for labeling. Free metal ions were eliminated by Sep-Pak C18 purification (Waters), using water. The metallopeptides were eluted with ethanol, evaporated to dryness, redissolved in water, and lyophilized.

Integrin $\alpha_v\beta_3$ Receptor Binding Assay

In vitro integrin-binding affinity for the metallopeptides was assessed via competitive cell binding assay in the human glioma cell line U87MG (American Type Culture Collection) using ^{125}I-echistatin as the radioligand, as previously described (*13,14*). Briefly, U87MG cells were seeded in 24-well plates (2×10^5 cells per well) and incubated overnight at 37°C/5% CO_2 in Dulbecco modified Eagle medium containing 10% fetal bovine serum. On the day of the experiment, the cells were rinsed twice with binding buffer (20 mmol of Tris per liter, pH 7.4, 150 mmol of NaCl per liter, 2 mmol of $CaCl_2$ per liter, 1 mmol of $MgCl_2$ per liter, 1 mmol of $MnCl_2$ per liter, and 0.1% bovine serum albumin) and incubated with ^{125}I-echistatin (30,000 cpm/well) in the presence of peptide (0–1,000 nmol/L) at RT for 2 h in a total volume of 300 μL. The supernatant was removed, and the cells were washed 3 times with cold binding buffer and were then collected with NaOH (1 mol/L). The cell-associated radioactivity was measured in a γ-counter. The

experiments were performed twice in triplicate for each peptide. The inhibitory concentration of 50% (IC_{50}) values were calculated by fitting the data by nonlinear regression using GraphPad Prism (GraphPad Software Inc.).

Determination of Lipophilicity

Each radiopeptide was added to a presaturated mixture of phosphate-buffered saline (pH 7.4)/octanol 1:1 at a concentration of 15 and 150 pmol/L ($n = 3$). The mixtures were vigorously shaken for 1 h and then centrifuged. The activity in 100 μL of both the phosphate-buffered saline and octanol phases were measured in a γ-counter, and the octanol-water partition coefficient (Log D) was calculated.

Animal Model and Biodistribution Studies

Animal experiments were performed according to the regulations of the University Hospital of Freiburg. Athymic nude female mice (age, 6–7 wk; weight, 16–18 g) were obtained from Charles River. U87MG cells were suspended in phosphate-buffered saline and Matrigel (BD Biosciences), injected subcutaneously into the right shoulder ($3–5 \times 10^6$ cells per mouse), and allowed to grow for 3–4 wk (tumor weight, 100–200 mg).

Mice were injected with 5 MBq/0.6 nmol/0.1 mL of ^{64}Cu-CB-TE2A-/NODAGA-/DOTA-c(RGDfK) or ^{68}Ga-NODAGA-/DOTA-c(RGDfK). Biodistribution of ^{64}Cu-labeled peptides was performed at 1 and 18 h after injection, and ^{68}Ga-labeled peptides were evaluated at 1 h after injection. Biodistribution studies with ^{64}Cu-NODAGA-c(RGDfK) were also performed at 4 h after injection. In addition, total-body radioactivity was measured for this compound by placing anesthetized mice ($n = 3$) in a dose calibrator immediately after injection and at 0.5, 1, 4, and 24 h after injection. The resulting whole-body time–activity curve was fitted by the sum of 2 exponential functions using the Prism software (GraphPad Software Inc.).

Nonspecific uptake was determined with coinjection of c(RGDfV) (5 mg/kg) and evaluated for all radiopeptides at 1 h after injection. Organs and blood were collected, rinsed of excess blood, blotted dry, weighed, and measured in a γ-counter. The radioactivity of the tissue samples was calibrated against a known aliquot of injected activity. Results were expressed as percentage injected activity per gram of tissue (%IA/g).

Small-Animal PET and Analysis

Animals were anesthetized with 1.5% isoflurane and imaged with a microPET Focus 120 scanner (Siemens Preclinical Solutions). Five megabecquerels (0.6 nmol) of radiopeptide were injected via lateral tail vein cannulation. The same amount of activity and peptide was used in both the imaging and the biodistribution studies to generate quantitative uptake data that accurately corresponded to the imaging studies. Twenty-minute static scans were acquired at 1 h after injection for ^{64}Cu- and ^{68}Ga-labeled peptides, and 45-min scans were acquired at 18 h after injection for ^{64}Cu-labeled peptides. PET images were reconstructed with an ordered-subset expectation maximization algorithm provided by the manufacturer. Image counts per pixel per second were calibrated to activity concentrations (Bq/mL) by measuring a 3.5-cm cylinder phantom filled with a known concentration of radioactivity. To determine tracer concentration in the tumors, ellipsoid regions of interest were placed in the area that exhibited the highest radioactivity as determined by visual inspection on micro-PET images generated by the AMIDE software (*15*). Regions of interest were then drawn on the side contralateral to the tumor to determine background uptake, and tumor-to-background ratios were generated using these values. Tracer uptake is expressed as percentage of decay-corrected %IA/g, with the color scale set from 0% to 3% for qualitative comparison among the images.

Statistical Analysis

Statistical analysis was performed by unpaired 2-tailed *t* test using Prism software (GraphPad Software Inc.). *P* values of less than 0.05 were considered significant.

RESULTS

Preparation of Radiotracers

The chemical structures of the conjugates are shown in Figure 1. The purity of each conjugate as determined by RP-HPLC was 97% or more. Labeling yields of ^{64}Cu and ^{68}Ga peptides were more than 97%. The specific activities ranged from 15 to 20 GBq/μmol for both radiometals. NODAGA-c(RGDfK) was labeled with ^{64}Cu and ^{68}Ga at RT within 10 min. For the other 2 conjugates, elevated temperature (95°C) and longer incubation time (≤30 min in the case of ^{64}Cu) were necessary for high labeling yields and specific activities.

In Vitro Characteristics of Radiometallopeptides

The receptor-binding affinity of the metallopeptides was compared with c(RGDfV) (reference molecule) using a competitive cell-binding assay (Supplemental Fig. 1; supplemental materials are available online only at http://jnm.snmjournals.org). All compounds inhibited the binding of ^{125}I-echistatin to $\alpha_v\beta_3$-positive U87MG cells in a dose-dependent manner. The IC_{50} values of ^{nat}Cu-CB-TE2A-c(RGDfK) and ^{nat}Cu-NODAGA-c(RGDfK) were similar to c(RGDfV) (4.5 ± 0.5, 6.5 ± 0.2, and $4.3 \pm 0.1 \times 10^{-7}$ mol/L, respectively), whereas a somewhat lower affinity was seen for ^{nat}Cu-DOTA-c(RGDfK) ($10.7 \pm 0.3 \times 10^{-7}$ mol/L). ^{nat}Ga-NODAGA-c(RGDfK) and ^{nat}Ga-DOTA-c(RGDfK) had IC_{50} values in the same range as the ^{nat}Cu-complexes (9.3 ± 0.4 and $7.0 \pm 0.2 \times 10^{-7}$ mol/L, respectively).

All ^{64}Cu-labeled peptides showed a similar hydrophilic character, with log D values of -2.92 ± 0.11, -2.76 ± 0.08, and -2.77 ± 0.10 for ^{64}Cu-CB-TE2A-c(RGDfK), ^{64}Cu-NODAGA-c(RGDfK), and ^{64}Cu-DOTA-c(RGDfK), respectively. ^{68}Ga-NODAGA-c(RGDfK) was more hydrophilic than ^{68}Ga-DOTA-c(RGDfK) (log D, -3.27 ± 0.01 and -2.86 ± 0.01, respectively).

Biodistribution Studies

The biodistribution data are summarized in Tables 1–3. All ^{64}Cu-labeled peptides had a similar tumor uptake, ranging between 3.7 and 4.0 %IA/g at 1 h after injection. Activity concentrations in normal organs were also similar with the exception of significantly higher liver uptake for the ^{64}Cu-DOTA-c(RGDfK) conjugate ($P < 0.01$). ^{64}Cu-NODAGA-c(RGDfK) and ^{64}Cu-CB-TE2A-c(RGDfK) demonstrated tumor-to-organ ratios greater than 1 for all organs except for the adrenal glands, which physiologically express $\alpha_v\beta_3$ integrins (*16*).

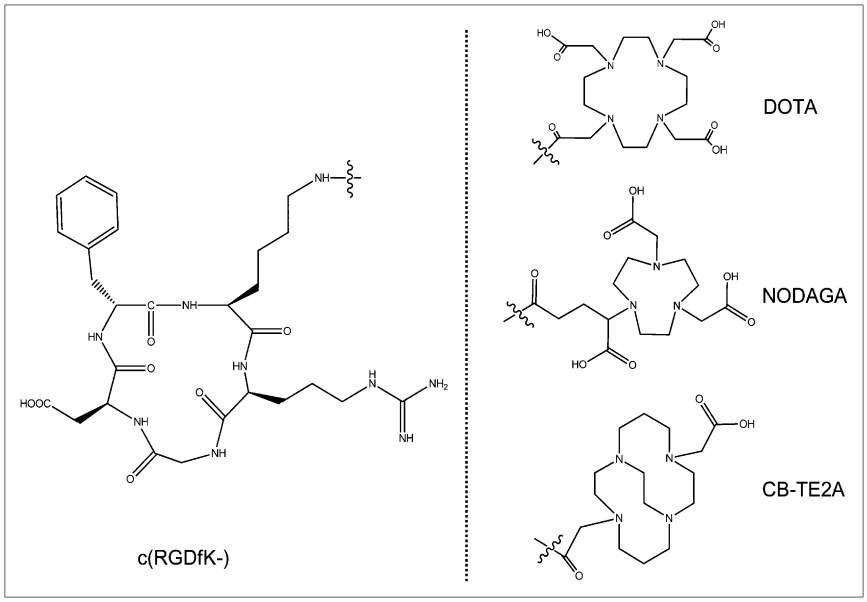

FIGURE 1. Structures of DOTA-c(RGDfK), NODAGA-c(RGDfK), and CB-TE2A-c(RGDfK).

At 18 h after injection, all ^{64}Cu-labeled peptides were retained in the tumor at a concentration of approximately 3 %IA/g (Table 2). In contrast, activity was cleared from all normal organs for ^{64}Cu-NODAGA-c(RGDfK) and ^{64}Cu-CB-TE2A-c(RGDfK), resulting in markedly improved tumor-to-organ ratios (Table 2; Fig. 2). For example, the tumor-to-blood ratio for ^{64}Cu-CB-TE2A-c(RGDfK) increased from 7.5 at 1 h to 146 at 18 h, tumor-to-liver ratio from 2.6 to 8.5, and tumor-to-intestine ratio from 2.8 to 3.8 (Fig. 2A). A similar improvement of tumor-to-organ ratios was observed for ^{64}Cu-NODAGA-c(RGDfK). In contrast, tumor-to-organ ratios improved only modestly for ^{64}Cu-DOTA-c(RGDfK) (Fig. 2).

The ease of radiolabeling and the favorable biodistribution made ^{64}Cu-NODAGA-c(RGDfK) the most promising compound of the 3 tested ^{64}Cu-labeled RGD peptides. We therefore studied the biodistribution of this compound in more detail. Whole-body measurements indicated that

TABLE 1
Biodistribution Results and Tumor–to–Normal Tissue Ratios of ^{64}Cu-CB-TE2A-c(RGDfK) in Nude Mice Bearing U87MG Tumors

Organ	1 h	1-h blocking*	18 h
Blood	0.49 ± 0.05	0.03 ± 0.01	0.02 ± 0.01
Heart	0.33 ± 0.11	0.04 ± 0.01	0.12 ± 0.05
Liver	1.57 ± 0.54	0.48 ± 0.10	0.37 ± 0.16
Spleen	1.33 ± 0.32	0.12 ± 0.03	0.63 ± 0.22
Lung	0.83 ± 0.21	0.14 ± 0.04	0.26 ± 0.07
Kidney	2.14 ± 0.53	1.18 ± 0.23	1.10 ± 0.38
Stomach	1.52 ± 0.63	0.15 ± 0.04	0.45 ± 0.14
Intestine	1.45 ± 0.55	0.30 ± 0.09	0.82 ± 0.19
Adrenal	2.63 ± 0.72	0.10 ± 0.04	1.45 ± 0.52
Pancreas	0.40 ± 0.25	0.09 ± 0.04	0.09 ± 0.04
Muscle	0.31 ± 0.13	0.02 ± 0.01	0.10 ± 0.03
Bone	2.57 ± 0.23	0.10 ± 0.01	0.22 ± 0.04
Tumor	3.66 ± 0.58	0.35 ± 0.29	2.99 ± 0.79
Tumor-to-nontumor ratios			
Tumor-to-blood	7.48 ± 0.90		146.07 ± 71.08
Tumor-to-liver	2.56 ± 1.06		8.47 ± 2.43
Tumor-to-kidney	1.87 ± 0.26		2.83 ± 0.80
Tumor-to-intestine	2.84 ± 1.22		3.75 ± 1.35
Tumor-to-muscles	13.61 ± 6.65		30.75 ± 2.03

*Coinjection of c(RGDfV) (5 mg/kg).
Data are %IA/g ± SD (n = 4–7).

TABLE 2
Biodistribution Results and Tumor–to–Normal Tissue Ratios of ^{64}Cu- and ^{68}Ga-NODAGA-c(RGDfK) in Nude Mice Bearing U87MG Tumors

Organ	^{64}Cu				^{68}Ga	
	1 h	1-h blocking*	4 h	18 h	1 h	1-h blocking*
Blood	0.31 ± 0.09	0.15 ± 0.03	0.10 ± 0.03	0.07 ± 0.01	0.16 ± 0.03	0.03 ± 0.01
Heart	0.43 ± 0.04	0.20 ± 0.08	0.29 ± 0.08	0.18 ± 0.04	0.33 ± 0.07	0.03 ± 0.01
Liver	1.67 ± 0.33	0.42 ± 0.14	1.03 ± 0.34	0.58 ± 0.20	1.86 ± 0.23	0.28 ± 0.04
Spleen	1.63 ± 0.42	0.38 ± 0.12	1.02 ± 0.12	0.50 ± 0.11	1.73 ± 0.44	0.15 ± 0.04
Lung	1.08 ± 0.09	0.23 ± 0.01	0.66 ± 0.22	0.38 ± 0.06	0.80 ± 0.07	0.09 ± 0.00
Kidney	2.21 ± 0.27	0.98 ± 0.03	1.57 ± 0.32	0.89 ± 0.23	1.98 ± 0.51	1.07 ± 0.19
Stomach	1.63 ± 0.43	0.49 ± 0.20	0.92 ± 0.20	0.54 ± 0.12	1.40 ± 0.34	0.19 ± 0.09
Intestine	2.12 ± 0.40	0.73 ± 0.19	1.26 ± 0.02	0.95 ± 0.22	1.83 ± 0.51	0.18 ± 0.05
Adrenal	4.67 ± 1.07	0.54 ± 0.15	3.47 ± 0.58	2.78 ± 1.26	5.88 ± 1.06	0.25 ± 0.10
Pancreas	0.53 ± 0.36	0.18 ± 0.09	0.21 ± 0.06	0.16 ± 0.02	0.23 ± 0.08	0.04 ± 0.01
Muscle	0.31 ± 0.03	0.44 ± 0.10	0.16 ± 0.03	0.10 ± 0.02	0.49 ± 0.29	0.07 ± 0.03
Bone	0.58 ± 0.08	0.33 ± 0.11	0.28 ± 0.06	0.34 ± 0.10	0.45 ± 0.21	0.08 ± 0.02
Tumor	3.77 ± 0.52	0.89 ± 0.10	3.62 ± 0.95	3.05 ± 0.62	5.19 ± 1.45	0.41 ± 0.11
Tumor-to-nontumor ratios						
Tumor-to-blood	10.15 ± 5.19		36.65 ± 6.46	50.69 ± 8.13	27.67 ± 7.01	
Tumor-to-liver	2.67 ± 0.53		3.75 ± 1.07	5.64 ± 1.47	2.75 ± 0.31	
Tumor-to-kidney	1.72 ± 0.24		2.37 ± 0.46	3.54 ± 0.67	2.64 ± 0.31	
Tumor-to-intestine	1.83 ± 0.46		2.88 ± 0.05	3.42 ± 1.23	2.87 ± 0.49	
Tumor-to-muscle	12.16 ± 1.48		23.34 ± 4.41	31.83 ± 3.17	12.80 ± 5.25	

*Coinjection of c(RGDfV) (5 mg/kg).
Data are %IA/g ± SD (n = 4–7).

75% of the radioactivity was cleared with a half-life of 15 min and 25% with a half-life of 6 h (Supplemental Fig. 3). Contrast between tumor and normal tissue increased 1–4 h after injection, and there was a further increase from 4–18 h after injection (Table 2; Supplemental Fig. 2). For example, tumor-to-liver ratios increased from 2.7 at 1 h after injection to 3.8 at 4 h after injection and to 5.6 at 18 h after injection.

In vivo uptake of the two ^{68}Ga-labeled peptides was comparable for most organs at 1 h after injection. After adrenals, the U87MG tumors were the tissue accumulating the highest amount of radioactivity (5.19 ± 1.45 %IA/g vs. 3.47 ± 0.78 %IA/g for ^{68}Ga-NODAGA-c(RGDfK) and ^{68}Ga-DOTA-c(RGDfK), respectively). The blood activity of ^{68}Ga-NODAGA-c(RGDfK) was significantly lower than that of ^{68}Ga-DOTA-c(RGDfK) (0.16 ± 0.03 %IA/g vs. 0.38 ± 0.07 %IA/g, P = 0.006), resulting in a higher tumor-to-blood ratio (27.7 vs. 9.2 for ^{68}Ga-NODAGA-c(RGDfK) and ^{68}Ga-DOTA-c(RGDfK), respectively). Additionally, a significantly improved tumor-to-kidney ratio was achieved for ^{68}Ga-NODAGA-c(RGDfK) versus ^{68}Ga-DOTA-c(RGDfK) (2.64 ± 0.31 vs. 1.57 ± 0.14, respectively, P = 0.002).

The coinjection of excess c(RGDfV) (5 mg/kg) with each radiotracer resulted in a significant reduction of tracer uptake by the U87MG tumors ($P < 0.01$), confirming the receptor-mediated uptake of the radiotracers in vivo (Tables 1–3). The coinjection of c(RGDfV) also reduced uptake in most normal organs studied (Tables 1–3).

Small-Animal PET

Small-animal PET images acquired at 1 and 18 h after injection confirmed the results of the biodistribution studies. The U87MG tumors were well visualized with all radiotracers at both time points (Figs. 3 and 4). At 1 h after injection, liver, kidney, intestine, and urinary bladder were also clearly visible on the PET images. Compared with ^{68}Ga-NODAGA-c(RGDfK), ^{68}Ga-DOTA-c(RGDfK) demonstrated higher blood-pool activity (Fig. 3), with a lower tumor-to-background ratio (11.97 ± 1.51 vs. 3.28 ± 1.38 for ^{68}Ga-NODAGA-c(RGDfK) and ^{68}Ga-DOTA-c(RGDfK), respectively). Liver and intestinal uptake was highest for ^{64}Cu-DOTA-c(RGDfK). Consequently, image contrast was lower for ^{64}Cu-DOTA-c(RGDfK) than for ^{64}Cu-NODAGA-c(RGDfK) and ^{64}Cu-CB-TE2A-c(RGDfK) (Fig. 4). At 18 h after injection, radioactivity had cleared from all organs for ^{64}Cu-NODAGA-c(RGDfK) and ^{64}Cu-CB-TE2A-c(RGDfK), resulting in low levels of background activity for both radiotracers and excellent image contrast, whereas there was only minor improvement in image contrast for ^{64}Cu-DOTA-c(RGDfK). This was reflected in the small-animal PET tumor-to-background ratios, which were 26.83 ± 3.52, 20.72 ± 5.59, and 7.61 ± 3.68 for ^{64}Cu-NODAGA-c(RGDfK), ^{64}Cu-CB-TE2A-c(RGDfK), and ^{64}Cu-DOTA-c(RGDfK), respectively (Fig. 4).

DISCUSSION

In this study, we performed a systematic comparison of ^{68}Ga- and ^{64}Cu-labeled RGD conjugates using 3 different

TABLE 3
Biodistribution Results and Tumor–to–Normal Tissue Ratios of ^{64}Cu- and ^{68}Ga-DOTA-c(RGDfK) in Nude Mice Bearing U87MG Tumors

Organ	^{64}Cu			^{68}Ga	
	1 h	1-h blocking*	18 h	1 h	1-h blocking*
Blood	0.63 ± 0.14	0.56 ± 0.23	0.42 ± 0.15	0.38 ± 0.07	0.60 ± 0.14
Heart	1.01 ± 0.21	0.70 ± 0.01	0.93 ± 0.16	0.35 ± 0.08	0.20 ± 0.05
Liver	5.46 ± 1.31	3.14 ± 0.44	2.59 ± 0.81	1.60 ± 0.27	0.48 ± 0.10
Spleen	1.71 ± 0.27	0.73 ± 0.01	1.30 ± 0.27	1.34 ± 0.21	0.36 ± 0.09
Lung	1.58 ± 0.30	2.38 ± 1.07	1.51 ± 0.44	0.87 ± 0.12	0.58 ± 0.11
Kidney	3.31 ± 0.12	2.96 ± 0.31	2.03 ± 0.65	2.24 ± 0.34	1.95 ± 0.68
Stomach	2.65 ± 0.50	1.31 ± 0.32	1.35 ± 0.62	1.50 ± 0.36	0.57 ± 0.11
Intestine	2.79 ± 0.52	1.40 ± 0.32	1.92 ± 0.58	1.79 ± 0.30	0.53 ± 0.08
Adrenal	4.02 ± 1.40	1.03 ± 0.24	2.31 ± 0.72	4.87 ± 1.21	0.71 ± 0.04
Pancreas	0.68 ± 0.08	0.34 ± 0.13	0.53 ± 0.15	0.29 ± 0.05	0.18 ± 0.01
Muscle	0.42 ± 0.08	0.23 ± 0.08	0.23 ± 0.01	0.29 ± 0.04	0.18 ± 0.02
Bone	0.53 ± 0.09	0.51 ± 0.08	0.39 ± 0.14	0.35 ± 0.05	0.11 ± 0.05
Tumor	3.97 ± 0.48	1.57 ± 0.13	3.23 ± 0.75	3.47 ± 0.78	0.89 ± 0.05
Tumor-to-nontumor ratios					
Tumor-to-blood	6.46 ± 1.57		8.30 ± 2.58	9.24 ± 1.12	
Tumor-to-liver	0.77 ± 0.24		1.35 ± 0.50	2.25 ± 0.37	
Tumor-to-kidney	1.20 ± 0.15		1.73 ± 0.65	1.57 ± 0.14	
Tumor-to-intestine	1.46 ± 0.29		1.82 ± 0.66	1.95 ± 0.16	
Tumor-to-muscles	9.94 ± 3.44		14.30 ± 0.40	12.37 ± 1.81	

*Coinjection of c(RGDfV) (5 mg/kg).
Data are %IA/g ± SD (n = 4–7).

chelating systems, CB-TE2A, NODAGA, and DOTA, with the aim of facilitating radiochemical synthesis of RGD-based PET radiotracers and improving in vivo imaging of $\alpha_v\beta_3$ integrins. The 2 key findings of our study can be summarized as follows: first, NODAGA is an attractive chelator for RGD peptides because radiolabeling with both ^{68}Ga and ^{64}Cu can be performed within 10 min at RT. Second, delayed imaging with ^{64}Cu-CB-TE2A-c(RGDfK) or ^{64}Cu-NODAGA-c(RGDfK) dramatically improves image contrast, because these compounds are only slowly cleared from $\alpha_v\beta_3$ integrin–expressing tumors, whereas their clearance from normal tissues is much faster. Furthermore, the clearance of the peptides from normal tissues is fast as compared with the physical half-life of ^{64}Cu and is expected to limit the radiation dose in humans.

The ^{64}Cu and ^{68}Ga conjugates presented here exhibited comparable in vitro affinity to $\alpha_v\beta_3$ integrins in a cell-binding assay (Supplemental Fig. 1). The resulting IC_{50} values are comparable to the reference molecule c(RGDfV) and to reported IC_{50} values of other RGD derivatives, such as galacto-RGD (IC_{50}, 4.0 ± 0.4 × 10^{-7} mol/L (*14*)) and others, studied in intact U87MG cells (*17,18*). The impact of the different chelators and radiometals on the integrin-binding affinity was thus modest, as has also been observed by other groups (*19–22*). IC_{50} values obtained from cell-based integrin-binding assays cannot be compared with those obtained from purified $\alpha_v\beta_3$ integrin fixed on a solid matrix, because cell-based assays consistently yield considerably higher IC_{50} values (*13,20*).

Consistent with their comparable affinity for the $\alpha_v\beta_3$ integrin, all studied compounds demonstrated a similar uptake in U87MG tumors at 1 h after injection. A tumor uptake of 3–4 %IA/g was observed—uptake that is comparable to that of previously reported monomeric ^{64}Cu- or

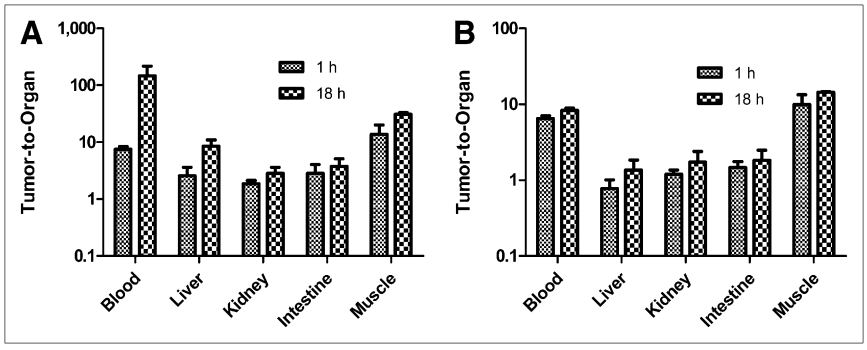

FIGURE 2. Tumor-to-organ ratios for ^{64}Cu-CB-TE2A-c(RGDfK) (A) and ^{64}Cu-DOTA-c(RGDfK) (B) at 1 and 18 h after injection. Graphs are in logarithmic scale.

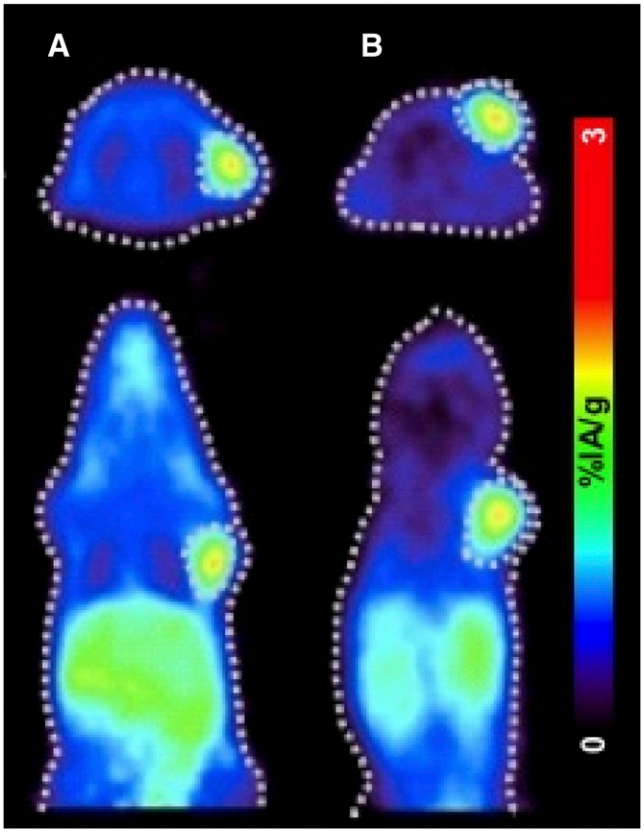

FIGURE 3. Transverse (top) and coronal (bottom) small-animal PET images of ^{68}Ga-DOTA-c(RGDfK) (A) and ^{68}Ga-NODAGA-c(RGDfK) (B) in nude mice bearing U87MG tumors at 1 h after injection.

^{68}Ga-labeled RGD peptides in $\alpha_v\beta_3$ integrin–expressing xenografts (*18,20,22,23*). Tumor uptake was significantly reduced by the coinjection of excess c(RGDfV), indicating receptor-specific binding in the tumor tissue. In the blocking studies, we also observed a significant reduction of tracer uptake in most normal tissues. This observation is in agreement with the literature, because, to our knowledge, all reported $\alpha_v\beta_3$ integrin imaging probes demonstrate low but blockable uptake in normal tissues (*18,20,22–24*). This may be because of the expression of low levels of $\alpha_v\beta_3$ or related integrins in normal tissues. However, further studies are needed to better characterize the binding of RGD peptides in normal murine tissues.

With respect to normal-tissue distribution at 1 h, there were some notable differences among the 5 tested compounds. First, ^{68}Ga-NODAGA-c(RGDfK) demonstrated a significantly (2-fold) lower blood radioactivity than ^{68}Ga-DOTA-c(RGDfK) at 1 h after injection. A relatively high blood radioactivity at 1 h has been observed previously for ^{68}Ga-DOTA-RGD peptides, as compared with ^{111}In-labeled RGD peptides (*20*). Next, a more marked difference in biodistribution was found for ^{64}Cu-DOTA-c(RGDfK) than for the 2 other ^{64}Cu-labeled peptides. At 1 h after injection, liver uptake of ^{64}Cu-DOTA-c(RGDfK) was more than 3-fold higher than uptake for ^{64}Cu-CB-TE2A-c(RGDfK) and ^{64}Cu-NODAGA-c(RGDfK). At 18 h after injection, liver uptake was 4.5- to 7-fold higher for ^{64}Cu-DOTA-c(RGDfK). The activity concentration in all other sampled normal tissues (except for the adrenals) was also higher for ^{64}Cu-DOTA-c(RGDfK) than for the other ^{64}Cu-labeled peptides (Tables 1–3). In the small-animal PET images, image contrast is greatly improved with the CB-TE2A and NODAGA conjugates at 1 h (Fig. 4).

The different in vivo behavior of ^{64}Cu-DOTA-c(RGDfK) is most likely a consequence of the limited in vivo stability of the ^{64}Cu-DOTA complex. Under physiologic conditions, Cu^{2+} may dissociate from the ^{64}Cu-DOTA conjugate and be transferred to copper-binding proteins (*25*), a phenomenon that could explain the relatively high blood and liver uptake. Conversely, the much lower blood and liver uptake values seen for ^{64}Cu-CB-TE2A-c(RGDfK) and ^{64}Cu-NODAGA-c(RGDfK) demonstrate the in vivo stability of these complexes. Other groups have also reported a pro-

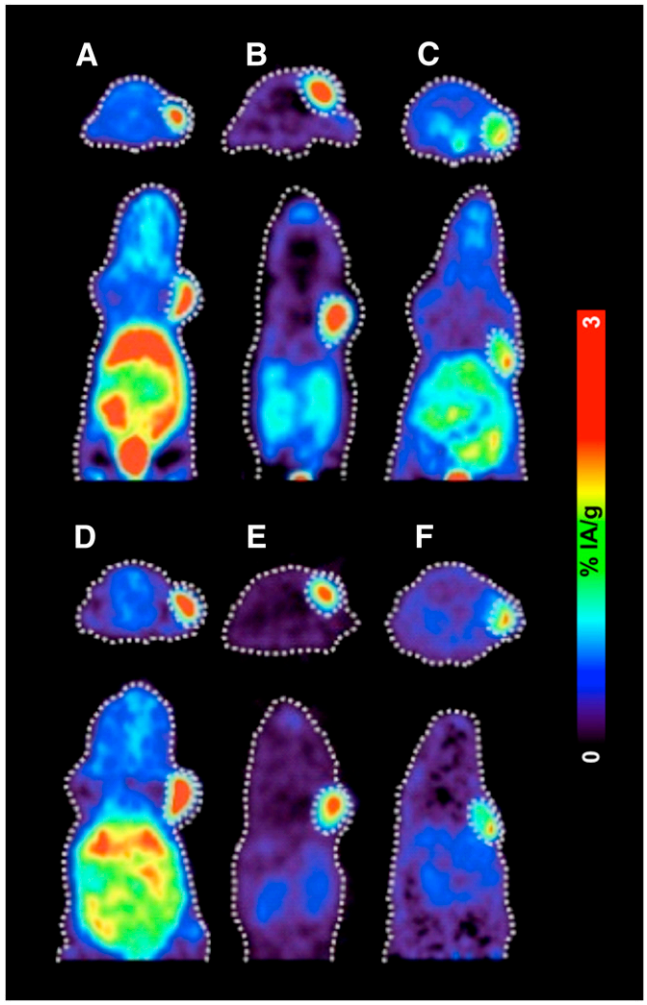

FIGURE 4. Small-animal PET images of ^{64}Cu-DOTA-c(RGDfK) at 1 h after injection (A) and 18 h after injection (D), ^{64}Cu-NODAGA-c(RGDfK) at 1 h after injection (B) and 18 h after injection (E), and ^{64}Cu-CB-TE2A-c(RGDfK) at 1 h after injection (C) and 18 h after injection (F) in nude mice bearing U87MG tumors.

longed liver and blood retention of ^{64}Cu-DOTA-RGD (*21,23,26*), and it has been shown that replacement of DOTA by more stable chelators for ^{64}Cu, such as sarcophagine-type chelators and CB-TE2A, improves biodistribution (*21,22*).

In the present study, tumor-to-background ratios steadily increased from 1 to 18 h after injection for ^{64}Cu-NODAGA-c(RGDfK). However, favorable tumor-to-background ratios were already obtained at 4 h after injection (Table 2). Because visualization of $\alpha_v\beta_3$ integrin–expressing tumors will depend both on tumor-to-background ratios and on counting rates, the optimum time for imaging with this ligand will depend on the location of the tumor, the sensitivity of the used PET scanner, and so on. Nevertheless, our data indicate that imaging at later times than feasible with ^{18}F or ^{68}Ga may be advantageous for visualization of $\alpha_v\beta_3$ integrin–expressing tumors.

In the present study, there was relatively little clearance of ^{64}Cu-DOTA-c(RGDfK) from U87MG xenografts during the first 18 h after injection (Table 3; Fig. 2). We have noted a similar slow clearance in 2 independent studies with U87MG and A431 xenografts (*27,28*). However, previous studies with the related peptide ^{64}Cu-DOTA-c(RGD**y**K) found a considerably faster tracer washout in U87MG xenografts (*21,23*). Similarly, ^{64}Cu-CB-TE2A-c(RGDfK) was retained longer in U87MG xenografts in the present study than previously reported for ^{64}Cu-CB-TE2A-c(RGD**y**K) (*22*). Future studies with head-to-head comparisons of c(RGDyK) and c(RGDfK) are necessary to confirm the longer intratumoral retention of c(RGDfK)-based imaging probes.

The tumor-to-organ ratios for ^{64}Cu-CB-TE2A-c(RGDfK) and ^{64}Cu-NODAGA-c(RGDfK) at 18 h after injection compare favorably with ^{18}F-galacto-RGD and with other previously described RGD peptides. In the present study, we observed tumor-to-muscle ratios of about 30, tumor-to-kidney ratios of 2.8–3.5, and tumor-to-liver ratios of 5.6–8 for these two ^{64}Cu-labeled peptides at 18 h after injection. In contrast, reported tumor-to-kidney and tumor-to-liver ratios for ^{18}F-galacto-RGD in murine tumor models are close to 1 (*20,29*). ^{18}F-labeled dimeric PEGylated RGD peptides provide improved tumor-to-liver ratios of about 4 for U87MG xenografts, and reported tumor-to-kidney ratios range between 1 and 2 (*30*). ^{68}Ga-labeled dimeric RGD peptides have demonstrated similar tumor-to-kidney ratios, with tumor-to-liver ratios of about 2 (*18,31*). Finally, PEGylated ^{64}Cu-DOTA-labeled dimeric RGD peptides have shown tumor-to-liver ratios of approximately 3 and tumor-to-kidney ratios of approximately 2 for U87MG tumors (*26*). Although this comparison with literature data is encouraging, we cannot exclude that the results are confounded by differences in the biodistribution across mouse strains or differences in $\alpha_v\beta_3$ expression levels by U87MG cells. Future studies are therefore warranted that perform a head-to-head comparison of the most promising ligands identified in this study (^{64}Cu/^{68}Ga-NODAGA-c(RGDfK)) with previously described ^{18}F- or ^{68}Ga-labeled RGD peptides.

To improve in vivo tumor uptake, several groups have developed radiolabeled tetra- and octameric RGDs (*13,14,18,24,26,30,31*). These multimeric RGDs showed significantly increased tumor uptake in vivo. Yet tumor-to-background contrast only modestly improves in the first 1–2 h after injection, because the multimeric RGDs show higher background activity due to slower blood clearance and increased kidney uptake (*14*). However, delayed imaging at 12–18 h after injection using multimeric RGD peptides stably labeled with ^{64}Cu-CB-TE2A/NODAGA may increase image contrast.

CONCLUSION

Our data strongly support the replacement of DOTA by CB-TE2A or NODAGA for radiolabeling of RGD peptides with ^{64}Cu or ^{68}Ga. Labeled CB-TE2A- or NODAGA-RGD peptides demonstrated an improved biodistribution in normal organs, resulting in significantly improved image contrast, especially for ^{64}Cu. In addition, NODAGA has the advantage of fast labeling under mild conditions. ^{68}Ga-NODAGA-RGD peptides can be produced conveniently on-site, independent of a nearby cyclotron facility, using a commercially available ^{68}Ge/^{68}Ga generator. Moreover, the straightforward synthesis can easily be performed in automatic modules. On the other hand, ^{64}Cu-RGDs could be produced centrally in accordance with good manufacturing practice requirements and sent to other sites for multicenter studies. Delayed imaging with ^{64}Cu-RGDs using the chelators NODAGA and CB-TE2A has significant potential to improve the visualization of $\alpha_v\beta_3$-positive tumors in vivo and may allow imaging of tumors with lower integrin expression levels than possible with ^{18}F- or ^{68}Ga-labeled RGD peptides. Because both ^{64}Cu- and ^{68}Ga-labeled RGD PET probes have specific advantages and disadvantages, their usefulness for specific clinical applications needs to be tested in human studies.

DISCLOSURE STATEMENT

The costs of publication of this article were defrayed in part by the payment of page charges. Therefore, and solely to indicate this fact, this article is hereby marked "advertisement" in accordance with 18 USC section 1734.

ACKNOWLEDGMENTS

We thank Dr. Jose Luis Sanchez for his assistance with the animal experiments. No potential conflict of interest relevant to this article was reported.

REFERENCES

1. Haubner R, Beer AJ, Wang H, Chen X. Positron emission tomography tracers for imaging angiogenesis. *Eur J Nucl Med Mol Imaging.* 2010;37(suppl 1):S86–S103.
2. Carmeliet P. Angiogenesis in life, disease and medicine. *Nature.* 2005;438:932–936.
3. Desgrosellier JS, Cheresh DA. Integrins in cancer: biological implications and therapeutic opportunities. *Nat Rev Cancer.* 2010;10:9–22.
4. Sipkins DA, Cheresh DA, Kazemi MR, Nevin LM, Bednarski MD, Li KC. Detection of tumor angiogenesis in vivo by alpha$_V$beta3-targeted magnetic resonance imaging. *Nat Med.* 1998;4:623–626.

5. Cai W, Niu G, Chen X. Imaging of integrins as biomarkers for tumor angiogenesis. *Curr Pharm Des.* 2008;14:2943–2973.
6. Haubner R, Weber WA, Beer AJ, et al. Noninvasive visualization of the activated alphavbeta3 integrin in cancer patients by positron emission tomography and [^{18}F]galacto-RGD. *PLoS Med.* 2005;2:e70.
7. Beer AJ, Schwaiger M. Imaging of integrin alphavbeta3 expression. *Cancer Metastasis Rev.* 2008;27:631–644.
8. Kenny LM, Coombes RC, Oulie I, et al. Phase I trial of the positron-emitting Arg-Gly-Asp (RGD) peptide radioligand ^{18}F-AH111585 in breast cancer patients. *J Nucl Med.* 2008;49:879–886.
9. Cho HJLJ, Park JY, Yun M, et al. First in human evaluation of a newly developed PET tracer, 18FRGD-K5 in patients with breast cancer: comparison with 18FFDG uptake pattern and microvessel density [abstract]. *J Nucl Med.* 2009;50(suppl 2):1910.
10. Fani M, Mueller A, Tamma ML, et al. Radiolabeled bicyclic somatostatin-based analogs: a novel class of potential radiotracers for SPECT/PET of neuroendocrine tumors. *J Nucl Med.* 2010;51:1771–1779.
11. Dai XSZ, Liu JO. An improved synthesis of a selective avb3-integrin antagonist cyclo(-RGDfK-). *Tetrahedron Lett.* 2000;41:6295–6298.
12. Eisenwiener KP, Prata MI, Buschmann I, et al. NODAGATOC, a new chelator-coupled somatostatin analogue labeled with [67/^{68}Ga] and [^{111}In] for SPECT, PET, and targeted therapeutic applications of somatostatin receptor (hsst2) expressing tumors. *Bioconjug Chem.* 2002;13:530–541.
13. Li ZB, Chen K, Chen X. ^{68}Ga-labeled multimeric RGD peptides for microPET imaging of integrin alpha$_v$beta$_3$ expression. *Eur J Nucl Med Mol Imaging.* 2008;35:1100–1108.
14. Liu S, Liu Z, Chen K, et al. ^{18}F-labeled galacto and PEGylated RGD dimers for PET imaging of alphavbeta3 integrin expression. *Mol Imaging Biol.* 2010;12:530–538.
15. Loening AM, Gambhir SS. AMIDE: a free software tool for multimodality medical image analysis. *Mol Imaging.* 2003;2:131–137.
16. Otis M, Campbell S, Payet MD, Gallo-Payet N. In adrenal glomerulosa cells, angiotensin II inhibits proliferation by interfering with fibronectin-integrin signaling. *Endocrinology.* 2008;149:3435–3445.
17. Maschauer S, Einsiedel J, Haubner R, et al. Labeling and glycosylation of peptides using click chemistry: a general approach to ^{18}F-glycopeptides as effective imaging probes for positron emission tomography. *Angew Chem Int Ed Engl.* 2010;49:976–979.
18. Dijkgraaf I, Yim C-B, Franssen GM, et al. PET imaging of alpha$_v$beta$_3$ integrin expression in tumours with ^{68}Ga-labelled mono-, di- and tetrameric RGD peptides. *Eur J Nucl Med Mol Imaging.* 2011;38:128–137.
19. Chen X, Park R, Hou Y, et al. MicroPET imaging of brain tumor angiogenesis with ^{18}F-labeled PEGylated RGD peptide. *Eur J Nucl Med Mol Imaging.* 2004;31:1081–1089.
20. Decristoforo C, Hernandez Gonzalez I, Carlsen J, et al. ^{68}Ga- and ^{111}In-labelled DOTA-RGD peptides for imaging of alphavbeta3 integrin expression. *Eur J Nucl Med Mol Imaging.* 2008;35:1507–1515.
21. Cai H, Li Z, Huang CW, et al. Evaluation of copper-64 labeled AmBaSar conjugated cyclic RGD peptide for improved MicroPET imaging of integrin alphavbeta3 expression. *Bioconjug Chem.* 2010;21:1417–1424.
22. Wei L, Ye Y, Wadas TJ, et al. ^{64}Cu-labeled CB-TE2A and diamsar-conjugated RGD peptide analogs for targeting angiogenesis: comparison of their biological activity. *Nucl Med Biol.* 2009;36:277–285.
23. Chen X, Hou Y, Tohme M, et al. Pegylated Arg-Gly-Asp peptide: ^{64}Cu labeling and PET imaging of brain tumor alphavbeta3-integrin expression. *J Nucl Med.* 2004;45:1776–1783.
24. Li ZB, Cai W, Cao Q, et al. ^{64}Cu-labeled tetrameric and octameric RGD peptides for small-animal PET of tumor alpha$_v$beta$_3$ integrin expression. *J Nucl Med.* 2007;48:1162–1171.
25. Wadas TJ, Wong EH, Weisman GR, Anderson CJ. Copper chelation chemistry and its role in copper radiopharmaceuticals. *Curr Pharm Des.* 2007;13:3–16.
26. Shi J, Kim YS, Zhai S, Liu Z, Chen X, Liu S. Improving tumor uptake and pharmacokinetics of ^{64}Cu-labeled cyclic RGD peptide dimers with Gly(3) and PEG(4) linkers. *Bioconjug Chem.* 2009;20:750–759.
27. Dumont RA, Hildebrandt I, Su H, et al. Noninvasive imaging of αvβ3 function as a predictor of the antimigratory and antiproliferative effects of dasatinib. *Cancer Res.* 2009;69:3173–3179.
28. Ferl GZ, Dumont RA, Hildebrandt IJ, et al. Derivation of a compartmental model for quantifying ^{64}Cu-DOTA-RGD kinetics in tumor-bearing mice. *J Nucl Med.* 2009;50:250–258.
29. Haubner R, Wester HJ, Weber WA, et al. Noninvasive imaging of alpha$_v$beta$_3$ integrin expression using ^{18}F-labeled RGD-containing glycopeptide and positron emission tomography. *Cancer Res.* 2001;61:1781–1785.
30. Liu Z, Liu S, Wang F, Chen X. Noninvasive imaging of tumor integrin expression using ^{18}F-labeled RGD dimer peptide with PEG (4) linkers. *Eur J Nucl Med Mol Imaging.* 2009;36:1296–1307.
31. Liu Z, Niu G, Shi J, Liu S, Wang F, Chen X. ^{68}Ga-labeled cyclic RGD dimers with Gly3 and PEG4 linkers: promising agents for tumor integrin alphavbeta3 PET imaging. *Eur J Nucl Med Mol Imaging.* 2009;36:947–957.

JNM The Journal of NUCLEAR MEDICINE

Novel ^{64}Cu- and ^{68}Ga-Labeled RGD Conjugates Show Improved PET Imaging of $\alpha_v\beta_3$ Integrin Expression and Facile Radiosynthesis

Rebecca A. Dumont, Friederike Deininger, Roland Haubner, Helmut R. Maecke, Wolfgang A. Weber and Melpomeni Fani

J Nucl Med. 2011;52:1276-1284.
Published online: July 15, 2011.
Doi: 10.2967/jnumed.111.087700

The Journal of Nuclear Medicine is published monthly.
SNMMI | Society of Nuclear Medicine and Molecular Imaging
1850 Samuel Morse Drive, Reston, VA 20190.
(Print ISSN: 0161-5505, Online ISSN: 2159-662X)

SNMMI SOCIETY OF NUCLEAR MEDICINE AND MOLECULAR IMAGING